Fluorescence Imaging

DNA Polyfluorophores for Real-Time Multicolor Tracking of Dynamic Biological Systems**

Shenliang Wang, Jia Guo, Toshikazu Ono, and Eric T. Kool

It is becoming widely appreciated that complex biological networks and interaction events need to be understood not only in the three spatial dimensions but also in the fourth dimension, time. To address this need, fluorescence imaging with light microscopy has entered a dynamic era. A series of time-lapsed images or an aggregated video of a dynamic event imparts much more information than a single still image, better revealing the natural organization and flow of biological processes. The widespread application of fluorescent proteins,[1] quantum dots,[2] and small-molecule fluorophores[3] in time-lapsed imaging, along with state-of-the-art optical technologies, such as super-resolution microscopy,[4] and integrated systems, such as intravital microscopy,[5] have aided enormous advances in understanding cellular and organismal biology. Tracking the movements of molecular and cellular targets has helped reveal processes such as metastasis,[6] secretory pathway cargo transfer,[1] and many more. The timeframe of the studied events can vary from hours to minutes, or even seconds.

Although it is possible to track sub-second motions by light microscopy, simultaneously tracking vectors of multiple species is hindered by the spectral limitations of common organic dyes and proteins, which require separate excitation wavelengths and emission filters. This drawback prevents the experimenter from recording visualization of multiple colors in real time, and thus most current multicolor labeling studies are based on post-image merging of multiple false-colored images. In moving systems, more complex imaging setups are required, including rapid filter wheel changes or multichannel imaging systems, increasing the complexity and cost of the instrumentation. Even with this added sophistication, timescales and numbers of colors are limited. Inorganic quantum dots can address this problem in part by taking advantage of a single UV excitation;[7] however, they present some of their own limitations as biological labels, including large size, multivalency, toxicity, and limited cellular permeability.[8]

Ideally, small-molecule, water-soluble organic dyes could be useful in multicolor dynamic imaging if they could be excited at one wavelength. In previous studies, we developed a new class of fluorescent dyes (oligodeoxyfluorosides (ODFs)) in which fluorescent aromatic species replace nucleobases in short DNA-like oligomers.[9] This molecular design has the advantage of rapid automated synthesis of thousands of possible composite dyes from a few components. In addition, the short DNA-like oligomers retain small size, are water-soluble, and are easily conjugated to small molecules and biomacromolecules.[10] An early study of a set of ODF fluorophores demonstrated multicolor emissions (in excess of ten colors) with single long wavelength UV excitation.[9] However, this first-generation set of dyes exhibited some limitations, such as low quantum yields of some monomers and oligomers, the chemical instability of one monomer, the rapid photooxidation of a benzopyrene component, and high toxicity of the benzopyrene starting material.[11] The dyes were not tested in dynamic systems. For more general multispectral applications, a set of single-excitation dyes might ideally exhibit similar levels of brightness, chemical and biological stability, and cell permeability.

To begin to address these issues, we designed and synthesized two new fluorescent deoxyriboside monomers. The extended pyrene monomer V (Figure 1a) was designed to substitute for a previous benzopyrene monomer by offering similar spectral characteristics, as well as the ability to form excimers in an aqueous environment.[12] The synthesis is shown in Scheme S1 of the Supporting Information, in addition details and spectral characterization are given. The superior fluorescent properties of a previous dicyanomethylene aminostyryl pyran monomer allowed us to retain the fluorophore while installing a more chemically stable link to the deoxyribose, giving the new monomer K (Figure 1a and Scheme S2 of the Supporting Information).

Incorporating these components, we prepared a candidate set of 18 ODF dyes using a DNA synthesizer (Figure 1c), and their absorption and fluorescence emission spectra were recorded (Figure 2). These ODFs can all be excited at 355 nm and cover the visible light range from blue to red. Quantum yields were above 25% for 13 of 18 dyes; fluorescence lifetimes ranged from 2.2 ns to more than 40 ns for the entire set (Table S1). The new V fluorophore (as SV; sequence given 5′->3′ with analogy to DNA) has a high quantum yield and emits strongly in the blue region. The monomers Y, E, and V are found to form excimers/exciplexes from cyan to green color (Figure 2 and Table S1) involving various combinations of the three aromatic monomers.

Incorporation of K monomer into the composite dyes greatly increased the ODF emission color range to yellow,

[*] Dr. S. Wang, Dr. J. Guo, Dr. T. Ono, Prof. Dr. E. T. Kool
Department of Chemistry, Stanford University
Stanford, CA 94305 (USA)
E-mail: kool@stanford.edu

Supporting information for this article such as details of synthetic procedures, optical measurements, additional data, details of fluorescent staining procedures, and additional imaging and video data is available on the WWW under http://dx.doi.org/10.1002/anie.201201928.
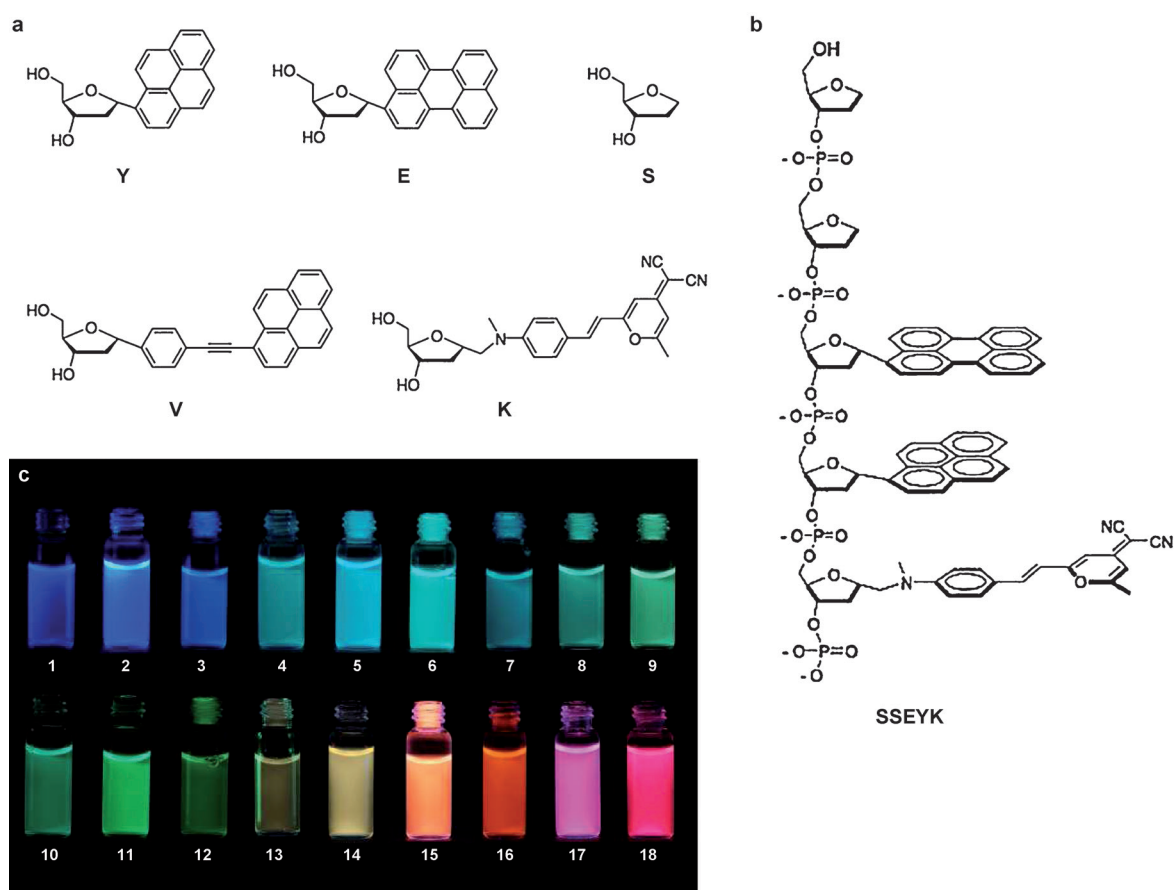
Figure 1. Molecular formulas and colors of ODF dyes in water. a) Monomer formulas; b) scheme of a representative ODF dye (SSEYK shown); c) images of aqueous solutions of ODFs under UV excitation (sequences 5′->3′): 1) SY, 2) SV, 3) SE, 4) SSSYYY, 5) SSEY, 6) SSYV, 7) SSEYE, 8) SSVEV, 9) SSVE, 10) SSYVE, 11) SSVV, 12) SSVVE, 13) SSEVE, 14) SSEYK, 15) SSVVK, 16) SSYKY, 17) SSVKV, 18) SSVKVK. One or more monomers lacking a fluorophore (S) are added to increase water solubility and inhibit aggregation. Illumination by UV lamp (>365 nm).

orange, and red wavelengths. Sequences containing both V and K monomers emit magenta hues, an effect of color addition of the blue and red wavelengths. For visual distinction in subsequent imaging experiments we chose the sequences SV (blue), SSEY (cyan), SSVV (green), SSEYK (yellow), and SSVKV (magenta/red) as a test set for further imaging experiments (see below).

Tracking labeled species over time requires that dyes possess sufficient photostability and biostability across the experimental timeframe. We measured spectra over a 2 h experiment (more than 20 minutes illumination time), evaluating the above five dyes along with FITC and Alexa 350 in phosphate buffered saline (PBS), as well as 10% human serum. One dye (SSVV) showed evidence of photobleaching (Figure S1), similar in rate to that of FITC. The remaining four ODF dyes exhibited little or no photobleaching. Interestingly, despite their phosphodiester backbones, none of the ODF dyes showed any evidence of biological degradation (e.g. by nucleases) in the serum solution over two hours (Figure S2), which suggests that the unnatural nucleobase structures are sufficient to confer nuclease resistance. Also, the dye SSVV displayed altered emission in serum

relative to PBS, suggesting an effect of protein binding on the dye conformation.

While the V monomer is photophysically quite stable (see data for the SV dye, Figure S3), we detected an interesting bleaching process of the VV dimer in the sequence SSVV. The 510 nm green emission, characteristic of an excimer state, is bleached at a rate similar to that of FITC. The monomer emission near 400 nm is unchanged. Neither pyrene alone (as Y) nor pyrene oligomers (as YY) exhibit this phenomenon, which suggests a major contribution of the ethynyl group in a photobleaching reaction. More work will be needed to shed light on this unusual bleaching mechanism. However, the SSEY sequence offers a photophysically stable alternative dye with a similar emission wavelength.

The most stable dyes (SV, SSEY, SSEYK, and SSVKV) were incubated with HeLa cells to evaluate their membrane permeability. The cultured cells were exposed to 2 μM dye in DMEM medium for 2 h at 37°C (Figure 3). The results confirm our earlier observations[9] that ODF dyes can successfully penetrate into the cells (showing predominantly cytoplasmic localization). The fact that they retain their emission colors in the intracellular environment (Figure 3) establishes that they are not degraded appreciably by
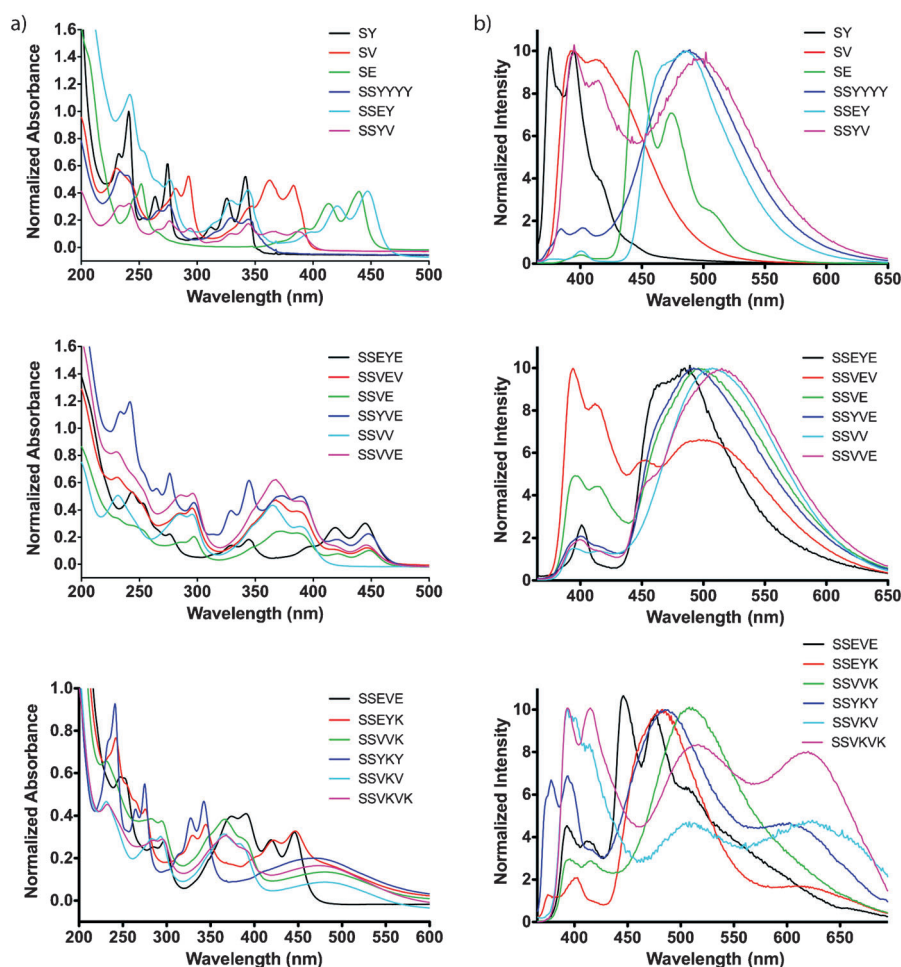
Figure 2. Normalized absorption (a) and emission (b) spectra of ODFs in this study. Emission spectra were recorded in water with 355 nm excitation.

nucleases over the time of the experiment. It is worth noting that the color of SSVKV in the HeLa cells shifted slightly closer to a true red color (as compared with its magenta hue in water, Figure 2).

As an initial test of applying ODF dyes in a dynamic system, we chose zebrafish (*Danio rerio*) embryos at one day post-fertilization. Embryos were separately stained in different ODF solutions (10 μM), rinsed with buffer and then mixed together for imaging. Although the oligomeric dyes did not penetrate the embryo chorion (except the blue SV dye), the outside of the chorion was vividly stained by the ODFs. The embryos were observed under an epifluorescence microscope and motions of developing fish inside the chorion were recorded in full color at 7 frames per second (fps; see Figure 4 and Supporting Information Video 1). In addition to the ODF staining, the embryos showed some yellowish autofluorescence background signal under the 340–380 nm wavelength excitation. Using a single excitation filter and capturing emission with a single, greater than 420 nm long-pass emission filter, the synchronous motions of embryos within the labeled chorion were monitored, showing the natural motions clearly on a subsecond timescale.

To provide a further test of the use of ODF dyes for monitoring separate moving targets, ODFs were applied to the invertebrate shrimp *Artemia salina*. The shrimp 1–2 days post-hatching were incubated with 10 μM ODFs in 1% NaCl solution for 4 h. After rinsing with 1% NaCl solution, the shrimp stained with differently colored dyes were mixed, and their motion was observed under an epifluorescence microscope (Figure 5 and Supporting Video 2). Although the shrimp were intentionally confined in their motions for imaging, their positions in each frame can be tracked and accurate moving traces could be recorded. Figure 5c shows four selected individuals with four different dye colors processed by the software Volocity, demonstrating the possibility of tracking four different targets by visual distinction as well as trace recording.

Next we moved to single-cell living targets for labeling, with the aim of attempting to track a greater number of moving components synchronously. We chose the ciliate protozoan *Paramecium caudatum*, which swims rapidly with spiral motion by way of coordinated cilia movements. The outer pellicle of the organism did not absorb ODF dyes, so we used an indirect staining approach, by dyeing their food. Yeast (*S. cerevisiae*) were heat-killed and separately stained with four different ODFs; the yeast were then fed to the protozoans for one hour. Under high magnification, the individual yeast cells are then visible in the cytoplasm of the *Paramecium* within food vacuoles (Figure 6). Using the lower-magnification 4× obective, approximately seventy moving *Paramecium* individuals, with four label colors, were present in the field of view, many moving over one body length on the 100 millisecond timescale (Supporting Information Video 3). Of these, eight *Paramecium* cells were selected and successfully tracked in an automated fashion. Their moving traces were processed, and are shown in Figure 5 f.

The experiments confirmed that the dye set SV, SSEY, SSEYK, and SSVKV allows the experimenter to visualize four label colors simultaneously with simple equipment. This not only captures motion in several colors very easily, but also simplifies multicolor still imaging. Still images such as in Figure 3 and 4 (top) could be seen directly by eye because they require no filter changes. This feature allows for the judgement of true colors and relative intensities for each species labeled with a given color. The relative brightness of this four-dye set is reasonably balanced (within about threefold across the series); this contrasts with inorganic
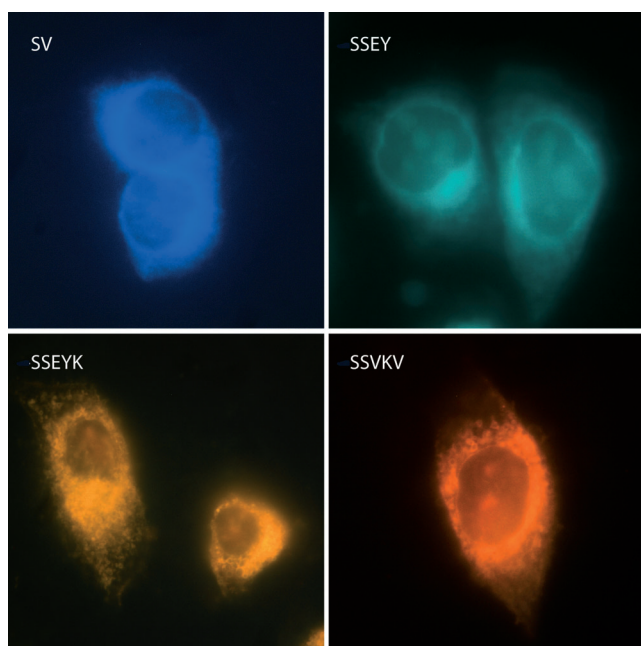
Figure 3. Epifluorescence microscope images of Hela cells stained with single ODF dyes (2 μM, 2 h incubation). Dye sequences are as shown (5′->3′). Images were taken with 340–380 nm excitation wavelength and a single long-pass filter (greater than 420 nm).
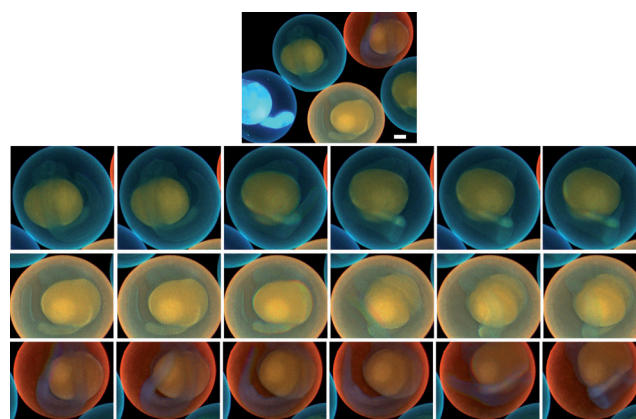

Figure 4. Still and video imaging of zebrafish embryos (*Danio rerio*), showing four-color (true color) labeling. Top: still image from the video showing four ODF dye colors in a single frame, without the need for recombination of separate false-colored images. Below: the three rows show six consecutive frames of the motion of each embryo within its chorion. Timespan of six frames is about 800 ms. Video was taken using 340–380 nm excitation wavelength and a single long-pass filter (greater than 420 nm) on an epifluorescence microscope. Dye sequences were: SV (blue), SSEY (cyan), SSEYK (yellow-orange), and SSVKV (red). See Supporting Information for the full video. Scale bar = 200 μm.

quantum dots (QD), which vary strongly in brightness across the color range.[13] Although inorganic QDs can exhibit high photostability, our data show that a set of ODFs can be stable against bleaching, even without antifade reagents, for over twenty minutes of cumulative UV illumination in air-saturated solutions.

Recent experiments in other groups have explored the unusual photophysical characteristics of multiple fluorophores organized by DNA.[14] Those approaches involve larger double-helical DNA structures, and few have been tested yet in biological systems. The current ODF molecules are distinct by being considerably smaller and single-
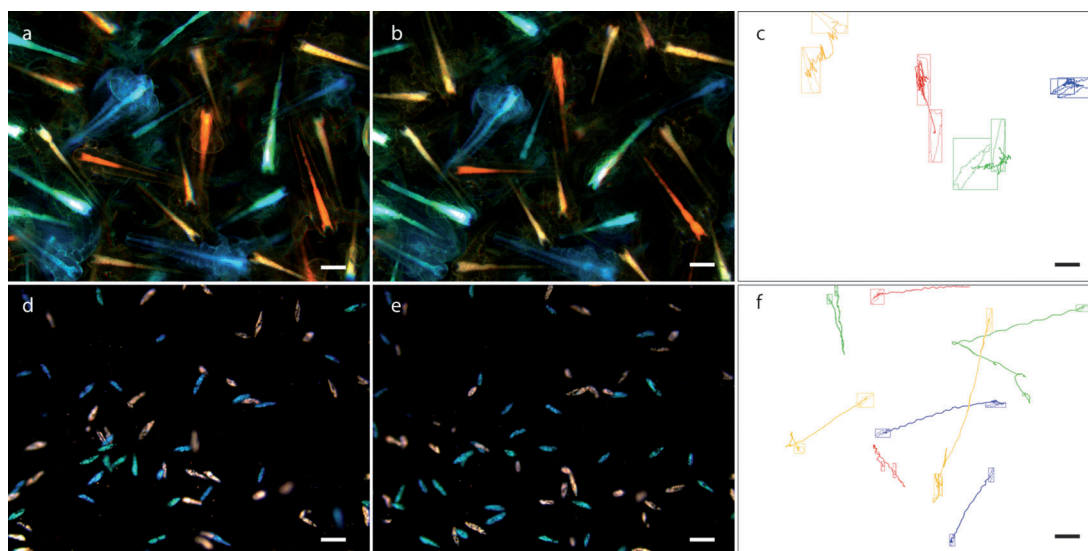

Figure 5. Tracking the motion of *Artemia salina* (a–c) and *Paramecium caudatum* (d–f) stained in four colors with ODF dyes. *Artemia salina* were stained with four ODFs (SV, SSEY, SSEYK, SSVKV) at 10 μM, 4 h. a) The first and b) last frame of a 14 s video and c) shows the tracking of the motions of four individuals, which are constrained by crowding. d–f) *Paramecium caudatum* were fed with yeast stained with ODFs (the same four dyes; see Figure 6 and Supporting Information for details). d) The first and e) last frame of a 10 s video and f) shows the automated tracking of the motion of eight individuals. Scale bar = 200 μm. Video was taken with 340–380 nm excitation wavelength and a single long-pass filter (greater than 420 nm) on an epifluorescence microscope. For full videos see Supporting Information.
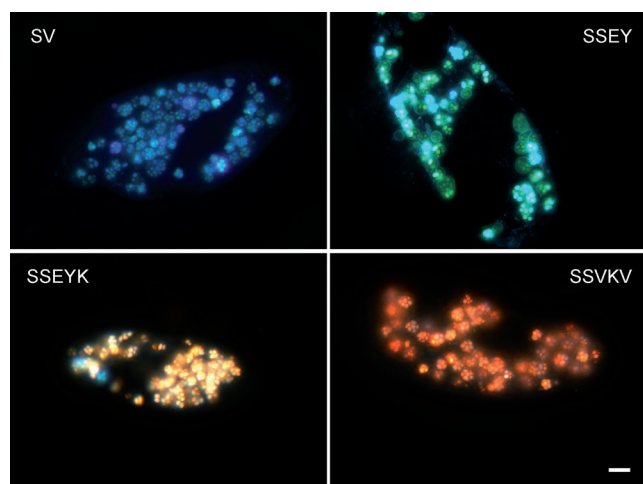
Figure 6. Epifluorescence microscope images of single *P. caudatum* cells fed with yeast stained with different ODF dyes (sequences shown). Scale bar = 20 μm. Images were taken with 340–380 nm excitation and a single long-pass filter (greater than 420 nm). Small groups of yeast cells are visible within food vacuoles of the *Paramecium*. See Figure S5 for bright-field image of *P. caudatum*.

stranded, which may confer benefits in cost, stability, and cell permeability.

The selected ODF dye set, SV, SSEY, SSEYK, and SSVKV, can be used as a fluorescent toolbox for blue, cyan, yellow, and red color labeling, respectively. Although the dyes were applied by direct staining without covalent conjugation, ODFs can be easily conjugated to small molecules and to antibodies if desired.[10] To our knowledge, the current results are an unprecedented demonstration of the use of small-molecule fluorescent dyes for multicolor simultaneous observation and tracking of rapid motions. Although we tested the application in a limited set of biological systems, we expect that such dyes could be used more broadly in biology and in other fields as well.

[1] J. F. Presley, N. B. Cole, T. A. Schroer, K. Hirschberg, K. J. Zaal, J. Lippincott-Schwartz, *Nature* **1997**, *389*, 81–85.

[2] a) A. B. Rosen, D. J. Kelly, A. J. Schuldt, J. Lu, I. A. Potapova, S. V. Doronin, K. J. Robichaud, R. B. Robinson, M. R. Rosen, P. R. Brink, G. R. Gaudette, I. S. Cohen, *Stem Cells* **2007**, *25*, 2128–2138; b) X. Gao, Y. Cui, R. M. Levenson, L. W. Chung, S. Nie, *Nat. Biotechnol.* **2004**, *22*, 969–976.

[3] a) S. T. Laughlin, J. M. Baskin, S. L. Amacher, C. R. Bertozzi, *Science* **2008**, *320*, 664–667; b) J. M. Baskin, K. W. Dehnert, S. T. Laughlin, S. L. Amacher, C. R. Bertozzi, *Proc. Natl. Acad. Sci. USA* **2010**, *107*, 10360–10365; c) N. Y. Kang, H. H. Ha, S. W. Yun, Y. H. Yu, Y. T. Chang, *Chem. Soc. Rev.* **2011**, *40*, 3613–3626.

[4] a) U. V. Nagerl, K. I. Willig, B. Hein, S. W. Hell, T. Bonhoeffer, *Proc. Natl. Acad. Sci. USA* **2008**, *105*, 18982–18987; b) J. Tønnesen, F. Nadrigny, K. I. Willig, R. Wedlich-Soldner, U. V. Nagerl, *Biophys. J.* **2011**, *101*, 2545–2552.

[5] M. J. Pittet, R. Weissleder, *Cell* **2011**, *147*, 983–991.

[6] E. Sahai, *Nat. Rev. Cancer* **2007**, *7*, 737–749.

[7] A. Sergé, N. Bertaux, H. Rigneault, D. Marguet, *Nat. Methods* **2008**, *5*, 687–694.

[8] a) U. Resch-Genger, M. Grabolle, S. Cavaliere-Jaricot, R. Nitschke, T. Nann, *Nat. Methods* **2008**, *5*, 763–775; b) A. M. Smith, S. Nie, *Nat. Biotechnol.* **2009**, *27*, 732–733; c) R. J. Byers, E. R. Hitchman, *Prog. Histochem. Cytochem.* **2011**, *45*, 201–237.

[9] a) Y. N. Teo, J. N. Wilson, E. T. Kool, *J. Am. Chem. Soc.* **2009**, *131*, 3923–3933; b) Y. N. Teo, Ph.D. Thesis, Stanford University (USA), **2010**.

[10] a) O. Khakshoor, E. T. Kool, *Chem. Commun.* **2011**, *47*, 7018–7024; b) N. Dai, E. T. Kool, *Chem. Soc. Rev.* **2011**, *40*, 5756–5770; c) J. Guo, S. Wang, N. Dai, Y. N. Teo, E. T. Kool, *Proc. Natl. Acad. Sci. USA* **2011**, *108*, 3493–3498.

[11] a) J. Gao, S. Watanabe, E. T. Kool, *J. Am. Chem. Soc.* **2004**, *126*, 12748–12749; b) J. Gao, Ph.D. Thesis, Stanford University (USA), **2004**.

[12] I. V. Astakhova, A. D. Malakhov, I. A. Stepanova, A. V. Ustinov, S. L. Bondarev, A. S. Paramonov, V. A. Korshun, *Bioconjugate Chem.* **2007**, *18*, 1972–1980.

[13] Y. Xing, Q. Chaudry, C. Shen, K. Y. Kong, H. E. Zhau, L. W. Chung, J. A. Petros, R. M. O'Regan, M. V. Yezhelyev, J. W. Simons, M. D. Wang, S. Nie, *Nat. Protoc.* **2007**, *2*, 1152–1165.

[14] a) E. Mayer-Enthart, H. A. Wagenknecht, *Angew. Chem.* **2006**, *118*, 3451–3453; *Angew. Chem. Int. Ed.* **2006**, *45*, 3372–3375; b) V. L. Malinovskii, F. Samain, R. Häner, *Angew. Chem.* **2007**, *119*, 4548–4551; *Angew. Chem. Int. Ed.* **2007**, *46*, 4464–4467; c) J. Chiba, S. Takeshima, K. Mishima, H. Maeda, Y. Nanai, K. Mizuno, M. Inouye, *Chem. Eur. J.* **2007**, *13*, 8124–8130; d) A. L. Benvin, Y. Creeger, G. W. Fisher, B. Ballou, A. S. Waggoner, B. A. Armitage, *J. Am. Chem. Soc.* **2007**, *129*, 2025–2034; e) I. V. Astakhova, V. A. Korshun, K. Jahn, J. Kjems, J. Wengel, *Bioconjugate Chem.* **2008**, *19*, 1995–2007; f) D. Baumstark, H. A. Wagenknecht, *Chem. Eur. J.* **2008**, *14*, 6640–6645; g) N. A. Grigorenko, C. J. Leumann, *Chem. Eur. J.* **2009**, *15*, 639–645; h) R. Varghese, H. A. Wagenknecht, *Chem. Eur. J.* **2009**, *15*, 9307–9310; i) A. L. Stadler, J. O. Delos Santos, E. S. Stensrud, A. Dembska, G. L. Silva, S. Liu, N. I. Shank, E. Kunttas-Tatli, C. J. Sobers, P. M. Gramlich, T. Carell, L. A. Peteanu, B. M. McCartney, B. A. Armitage, *Bioconjugate Chem.* **2011**, *22*, 1491–1502; j) F. Garo, R. Häner, *Angew. Chem.* **2012**, *124*, 940–943; *Angew. Chem. Int. Ed.* **2012**, *51*, 916–919.